2

Drag Measurement of a Complete Aircraft Model in Wind Tunnel Testing

Nobuyuki TSUBOI, Takeshi KAIDEN, Hideki NOMOTO, Masaru KODAMA and Keiji SATO
Mitsubishi Heavy Industries, Ltd. , Nagoya, Japan
and
Takashi YOSHINAGA, Junichi NODA, Hideo SEKINE, Atsushi TATE and Mitsunori WATANABE
National Aerospace Laboratory, Tokyo, Japan

1 Introduction

National Aerospace Laboratory and Mitsubishi Heavy Industries executed a series of research on high speed wind tunnel testing of a scale model of a supersonic transport aircraft from 1992 to 1994. The research history for those three years is shown in Figure 1. In 1992, wind tunnel testing of a complete aircraft was conducted to obtain basic aerodynamic characteristics at supersonic speeds. As a result, it was found that the neutral point moved backward approximately 6 % at $M = 2.0$ when no trim was taken. In 1993, based on the above result, wind tunnel testing for stabilizer control effectiveness was conducted to schedule the center of gravity in order to eliminate any drag increment due to trim. However, the maximum lift to drag ratio(at $M = 2.0$, with trim, corrected to actual size) obtained in 1992 and 1993 was 7.2, which is not higher than that of the Concorde. One of the causes was thought to be a spillage forward of the nacelles as a result of oil flow testing in 1992. Hence, in 1994, wind tunnel testing was conducted to investigate the cause of the spillage. The purpose of this paper is to report the results, by year, of the research conducted from 1992 to 1994.

2 Wind Tunnel Testing in 1992

2.1 Purpose of the Wind Tunnel Testing

- Evaluation of Basic Aerodynamic Characteristics at Supersonic Speed

2.2 Test Conditions

(1) Wind Tunnel
- Supersonic Wind Tunnel of National Aerospace Laboratory

(2) Flow Conditions
- $M = 1.4, 1.7, 2.0$
- $\alpha = -2° \sim 12°$
- $\beta = 0°, 5°$
- $Re = 6.3 \sim 7.3 \times 10^6$ (Based on M.A.C.)

(3) Measurement
- Six-Component Forces of a Complete Aircraft Configuration
- Oil Flow on Upper and Lower Surface of Main Wing
- Static and Total Pressure at Nacelle Nozzle Exit
- Schlieren Photograph around a Complete Aircraft

(4) Wind Tunnel Test Model

The wind tunnel test model is based on the supersonic transport configuration[1] with a horizontal tail as a result of the study in 1991 conducted by Mitsubishi Heavy Industries. The model outline drawing is shown in Figure 2 and the model installation concept in the wind tunnel is shown in Figure 3.

2.3 Results and Discussions

(1) Results of Six-Component Forces

The lift to drag ratio $(L/D) \sim CL$ curve at $M = 2.0$ is shown in Figure 4. It is understood that the maximum lift to drag ratio (with no trim, corrected to actual size) at cruise Mach number (2.0) is 7.3 at $CL = 0.125$. Since the maximum lift to drag ratio of the Concorde is 7.3 ($M = 2.05$)[2] , the lift to drag ratio of the proposed configuration is equal to that of the Concorde. The neutral point calculated from the results of the wind tunnel testing is shown in Figure 5. It is 61.4 % M.A.C. at $M = 0.6$ but it moves backward approximately 6 % at supersonic speeds. Since some trim drag increment and some maximum lift to drag ratio reduction are included by the neutral point moving backward, the center of gravity position should be scheduled to prevent the trim drag increment.

(2) Results of Flow Visualization

A Schlieren photograph at $M = 2.0$ is shown in Figure 6. In this photograph, it can be seen that a shock wave propagates from the nacelle on the under surface of the model to the rear of the model. It is considered that the shock wave is generated at the external compression type air intake.

(3) Results of Oil Flow

Oil flow testing results at $M = 2.0$ is shown in Figure 7. It is considered that the oil flow pattern in front of the nacelle is due to spillage, which results in reduction of the lift to drag ratio.

2.4 Summary

Results of wind tunnel testing in 1992 are summarized as follows:

(1) The basic aerodynamic characteristics of a complete aircraft at supersonic speed was obtained and the maximum lift to drag ratio of 7.3 (with no trim, corrected to actual size) at $M = 2.0$ was acquired.

(2) The neutral point at supersonic speed moves backward approximately 6 % in comparison with that at subsonic speed.

(3) Oil Flow testing around the nacelle at supersonic cruise speed shows that spillage occurs at the air intake.

Therefore, it was determined that in order to prevent any trim drag increment, wind tunnel testing acquire data on the stabilizer control effectiveness for the optimum center of gravity position should be conducted in 1993.

3 Wind Tunnel Testing in 1993

3.1 Purpose of the Wind Tunnel Testing

- Acquisition of the Stabilizer Control Effectiveness

3.2 Test Conditions

(1) Wind Tunnel
- Supersonic Wind Tunnel of National Aerospace Laboratory

(2) Flow Conditions
- $M = 1.4, 1.7, 2.0$
- $\alpha = -2^\circ \sim 12^\circ$
- $\beta = 0^\circ$
- $Re = 6.3 \sim 7.3 \times 10^6$ (Based on M.A.C.)

(3) Measurement
- Six-Component Forces of a Complete Aircraft Configuration
- Schlieren Photograph around a Complete Aircraft

(4) Wind Tunnel Test Model

The strut sting shown in Figure 8 was fabricated in order to deflect the stabilizer at both positive and negative angles.

3.3 Results and Discussions

(1) Results of Six-Component Forces

Pitching moment coefficient versus stabilizer deflection angle is shown in Figure 9. From the fact that the difference ΔCm at negative deflection angles from Cm with $\delta h = 0^\circ$ is higher than that at positive deflection angles, it is understood that the control effectiveness at a negative deflection angle is higher than that at a positive one. For the above reason, it is considered that since the fairing is provided on the fuselage aft under surface, the flow from the aircraft under surface to the upper surface is included and thus control effectiveness at positive deflection angles is reduced.

(2) Results of Calculation of Optimum Center of Gravity

Figure 10 shows the relation between drag coefficient at 1G trim and center of gravity at various Mach numbers. Maximum lift to drag ratio on the trim flight at $M = 2.0$ is 7.2. Optimum centers of gravity that minimize the trim drag are nearly 66 % at any Mach number. As a result of the arithmetic averaging of the optimum centers of gravity at $M = 1.7$ and 2.0, those at speeds of $M = 1.5 \sim 2.0$ are determined to be 66.5 % (Figure 11).

Figure 12 shows lift to drag ratio with and without a longitudinal stability compensation control. Without longitudinal stability compensation control, the longitudinal stability is negative with the center of gravity of 66.5 %. Hence, in order to provide positive longitudinal stability without compensation control, the center of gravity should be 20.1 % forward from the position where the trim drag is minimum, and thus the lift to drag ratio should be decreased to 5.4. On the other hand, with compensation control, the center of gravity can be located at the optimum position and thus the lift to drag ratio can be improve by 1.8 over than without such control. Hence, it can be said that the use of longitudinal stability compensation control is an effective means to improve lift to drag ratio.

3.4 Summary

Results of wind tunnel testing in 1993 are summarized as follows:

(1) The stabilizer control effectiveness was acquired and the optimum center of gravity was obtained.

(2) The maximum lift to drag ratio of 7.2 at $M = 2.0$ (with trim, corrected to actual size) was obtained.

(3) It could be confirmed that the longitudinal stability compensation control was effective for improvement of lift to drag ratio.

As a result of the 1993 tests, the lift to drag with trim could be acquired by stabilizer control effectiveness at supersonic cruise speed. Hence, it was determined that the spillage phenomenon in front of the nacelle (refer to the oil flow testing results in 1992) that was considered to be a cause of drag increment, should be investigated in 1994 in order to improve lift to drag ratio.

4 Wind Tunnel Testing in 1994

4.1 Purpose of the Wind Tunnel Testing

- Investigation of the Spillage in front of the Nacelle
- Evaluation of the Effect of Azimuthal Angle of Nacelle

4.2 Background of Wind Tunnel Testing

As a result of oil flow tests in 1992, spillage was observed in front of the nacelle on the wing under surface. The cause has been thought to be that the boundary layer flows into the nacelle inside, the flow is choked in the nacelle and the spillage consequently occurs since the diverter height is less than the boundary layer thickness δ on the wing surface (estimated using the Van-Driest method) at the wind tunnel testing Reynolds number. Therefore, the cause of the spillage in front of the nacelle should be investigated by using various diverter heights taller than the boundary layer thickness.

On the other hand, changing the azimuthal angle of the nacelle can be considered as one method to reduce drag of complete aircraft due to the wing/nacelle interaction[3]. The nacelles in this configuration were attached to the wing in parallel to the body axis. But as a result of wind tunnel testing in 1992, the flow around the nacelles on the wing under surface had some azimuthal angles in the spanwise direction and their angles were approximately 1.8° for the inboard nacelle and 3.0° for the outboard nacelle. Since those are considered to be the cause of drag increment, the possibility of reducing the drag of the complete aircraft should be investigated by changing the axis of the nacelle so that they are parallel to the out flow on the wing under surface.

Based on the above background, the wind tunnel testing was conducted.

4.3 Test Conditions

(1) Wind Tunnel
- Supersonic Wind Tunnel of National Aerospace Laboratory

(2) Flow Conditions
- $M = 2.0$
- $\alpha = -2° \sim 12°$
- $\beta = 0°$
- $Re = 7.3 \times 10^6$ (Based on M.A.C.)

(3) Measurement
- Six-Component Forces of a Complete Aircraft Configuration
- Oil Flow on Lower Surface of Main Wing
- Static and Total Pressure at Nacelle Nozzle Exit
- Schlieren Photograph around Complete Aircraft

(4) Wind Tunnel Test Model

In order to conduct (i) the change of diverter height and (ii) the change of azimuthal angle of nacelle based on the model used in 1992 and 1993, some spacers of the same plane figure as the diverter were fabricated to change the height and the azimuthal angel by being inserted between the diverter and the wing(Figure 13).

4.4 Results and Discussions

(1) Effect of Diverter Height

(a) Oil Flow Results

(i) Oil Flow on the Wing under Surface

Figure 14 shows results of oil flow around the nacelles on the wing under surface with various diverter heights. As the case of the original diverter height (Figure 14(a)) and the case of the diverter height equal to δ (boundary layer thickness on wing at air intake)(Figure 14(b)) are compared with each other, the oil flow patterns between the inboard and outboard nacelle are different from each other. It is considered that the compression waves generated by the interaction between the nacelle and the boundary layer affect the flow on the wing under surface. When a diverter height of δ (Figure 14(b)) a diverter height of 5 δ (Figure 14 (c)) are compared with each other, it can be seen that the separation line between the left and right inboard nacelles for the latter is wider than that for the former. But it is considered that the oil flow patterns around the nacelles are not affected so much even though the diverter height is changed.

Next, testing with closed nacelle exits was conducted to investigate whether the choking existed in the nacelle internal flow. The separation line with closed nacelle exits (Figure 14(d) left) is moved farther upstream than with opened nacelle exits (Figure 14(d) right), and also the flow patterns between the inboard and outboard nacelles are much different. From the above fact, it is thought that the nacelle internal flow is not choked even at the original diverter height.

(ii) Oil Flow on the Side of Nacelle

Figure 15 shows the results of oil flow on the side of the nacelle in case of various diverter heights. With the original diverter height (Figure 15(a)), the shock wave reflection traces are seen on the side of the inboard nacelle and those traces are also seen both when the diverter height is equal to δ (Figure 15(b)) and when it is equal to 5δ (Figure 15(c)). Hence, it can be said that diverter height variation has no influence on the oil flow pattern on the side of the nacelle.

(b) Mass Flow Ratio of Nacelle Internal Flow

Mass flow ratio of nacelle internal flow is calculated from the total pressure in the nacelle using Rayleigh's formula for pitot tubes. As a result, with the original diverter height for which it was considered that the nacelle internal flow might be choked due to the wing surface boundary layer flowing into the nacelle, the mass flow ratio of nacelle internal flow at $\alpha = 0°$ was 92 % (obtained in 1992). But even when the diverter height was 5δ (this obviously was assuming that the wing surface boundary layer did not go into the nacelle

and thus the nacelle internal flow was not choked), the mass flow ratio of nacelle internal flow at $\alpha = 0°$ was 94 %. Therefore, it is considered that the nacelle internal flow is not choked and flows sufficiently.

As a result of the wind tunnel testing with various diverter heights, it is found that flow goes sufficiently in the nacelle with the original diverter height. So, it can be concluded that the oil flow pattern on the wing under surface is not affected by spillage generated due to choking in the nacelle.

(2) Effect of Change of Nacelle Azimuthal Angle

Figure 16 shows ΔC_{D0} with various nacelle azimuthal angles. When the nacelle azimuthal angle was changed, with diverter heights of 2δ and 5δ , the variation of drag coefficient is a few counts and no significant effect of nacelle azimuthal angle was observed. It is considered that since base drag generated at the aft end of the diverter was large, the effect of change of nacelle azimuthal angle could not be captured.

(3) Study of the Flowfield Structure near the Nacelle

According to the results in paragraph (1), it is found that the oil flow pattern observed with the original diverter height is not separated shock wave caused by choking in the nacelle. Hence, the flowfield structure near the nacelle is studied in detail since the oil flow pattern is considered to be caused by physical phenomenon which is the interaction between the shock wave and the boundary layer.

(a) Flowfield with the Interaction between Shock Wave and Boundary Layer

When a wedge on a flat plate is placed in a supersonic flow (Figure 17), it is well known that a significant physical phenomenon can be observed[3,4]. That is, the shock wave near the flat plate bifurcates into a separation shock wave and a rear shock wave due to the interaction with the boundary layer on the flat plate, and consequently forms a λ shaped shock wave. The boundary layer separates from the flat plate at S1 due to the interaction with the separation shock wave. The separated shock flow is accelerated by expansion waves (which are generated due to the rear shock wave interacting with the separated boundary layer) between contact discontinuity and the separated boundary layer passing through the rear shock wave. The accelerated flow impinges upon the flat plate at A1 but some flow is directed back upstream. This reserve flow then encounters secondary separation at S2. Hence, separation lines of S1 and S2, and the attachment line A1 should be seen in oil flow testing.

(b) Flowfield near the Nacelle

Figure 18 shows results of oil flow on the wing under surface with the diverter height of δ. Primary separation line S1 and secondary separation line S2 similar to those in Figure 17 which, it is supposed, occur due to the interaction between the shock wave generated at air intake and the boundary layer, can be seen on the wing under surface. But the attachment line can not clearly be seen in Figure 18. The separation line S3, which are made by combining S1 and S2, can be seen between the inboard and outboard nacelles. In Figure 18, shock wave traces D can be seen on the lower surfaces of the inboard and outboard nacelles. Similar traces can be seen on the side of the nacelle (Figure 19 (a)). These traces are considered to be made by the shock wave from the air intake (Figure 19(b)).

By the above results, it is found that the oil flow pattern on the wing under surface is due to the complicated interaction between the shock waves from the nacelles and the boundary layer.

4.5 Summary

Results of wind tunnel testing in 1994 are summarized as follows:

(1) It is considered that the oil flow pattern in front of the nacelle is not caused by the spillage but rather by the complicated interaction between the shock waves from the nacelle and the boundary layer on the wing under surface.

   (a) No essential change of oil flow pattern can be seen with various diverter heights and it can be concluded that the spillage is a small amount even with the original diverter height judging from the mass flow ratio of the nacelle internal flow.

   (b) As the oil flow results in the wind tunnel testing are compared with the structure of the flowfield for a wedge mounted on a flat plate at supersonic speed, it can be concluded that the oil flow pattern in front of the nacelle is due to the interaction between the shock waves from the nacelle and the flat plate boundary layer.

(2) Little effect on the drag of the complete aircraft with various azimuthal angles of nacelle is obtained in this wind tunnel testing.

5 Conclusions

High speed wind tunnel testing using a full configuration scale model of a supersonic transport and the evaluation of its aerodynamic characteristics were conducted from 1992 to 1994. As a result, it is concluded that even a small scale model investigation of aerodynamic characteristics can be performed. It is considered that more wind tunnel testing needs to be conducted using lager models to realize improvement of the aerodynamic characteristics of the supersonic transport.

References

[1] Takami, H. and Kawashima, E., "Aerodynamic Characteristics of a Next Generation High-Speed Civil Transport," AIAA Paper 92-4229, 1992.

[2] Collard, D., "Concorde Airframe Design and Development," SAE912162.

[3] Landum, E. J., "Effect of Nacelle Orientation on the Aerodynamic Characteristics of an Arrow Wing-Body Configuration at Mach Number 2.03,' NASA TN D-3284, 1966.

[4] Knight, D. D. and Horstman, C. C., "Structure of Supersonic Turbulent Flow Past a Shape Fin," AIAA J Vol.25, No.10, p.1331-1337, 1987.

[5] Schmisseur, J. D. and Dolling, D. S., "Actual Wall Pressure near Separation in Highly Swept Turbulent Interactions," AIAA J. Vol.32, No.6, p.1151-1157, 1994.

Item \ Year	1992	1993	1994
Estimation of Basic Aerodynamic Characteristics	←	→	
Aquisition of Stabilizer Control Effectiveness		←	→
Estimation of Wing/Nacelle Interaction			← →

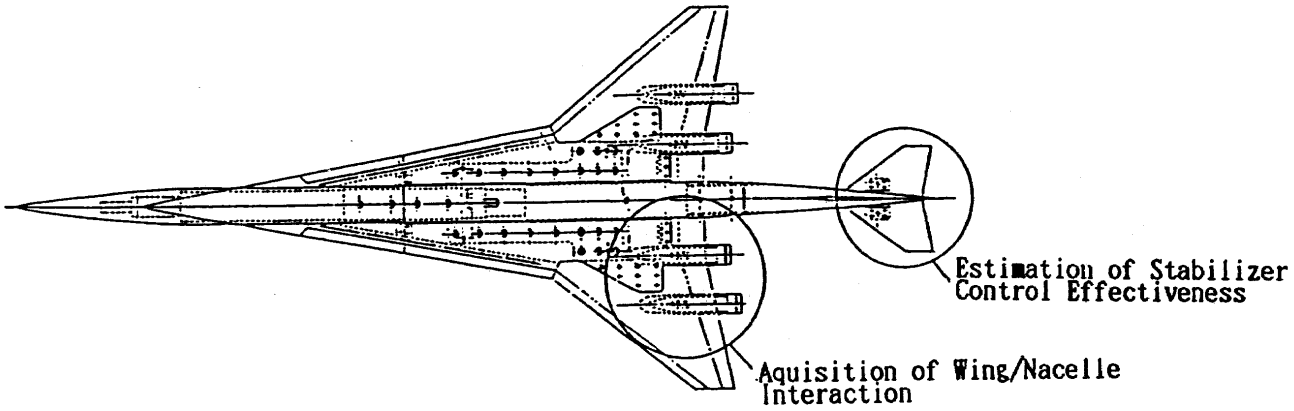

Figure 1 Research History for 3 Years

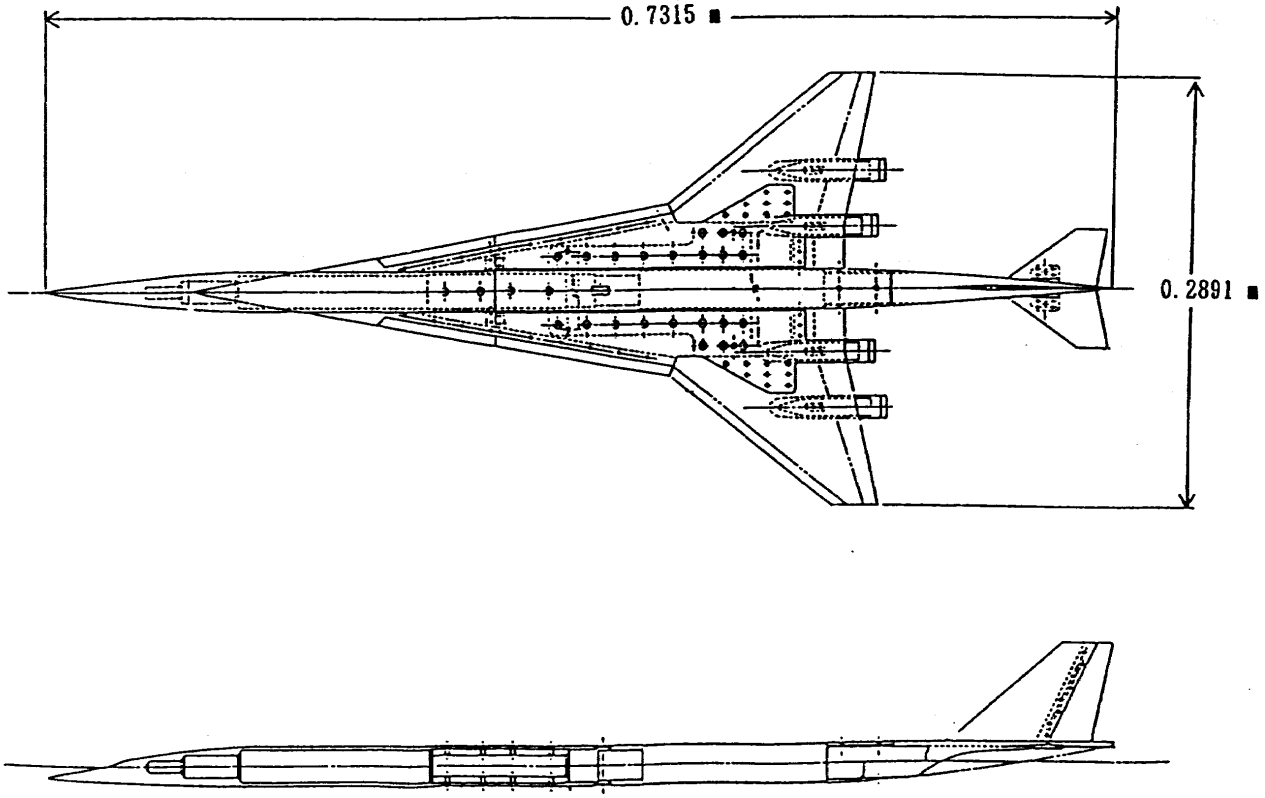

Figure 2 Model Outline Drawing

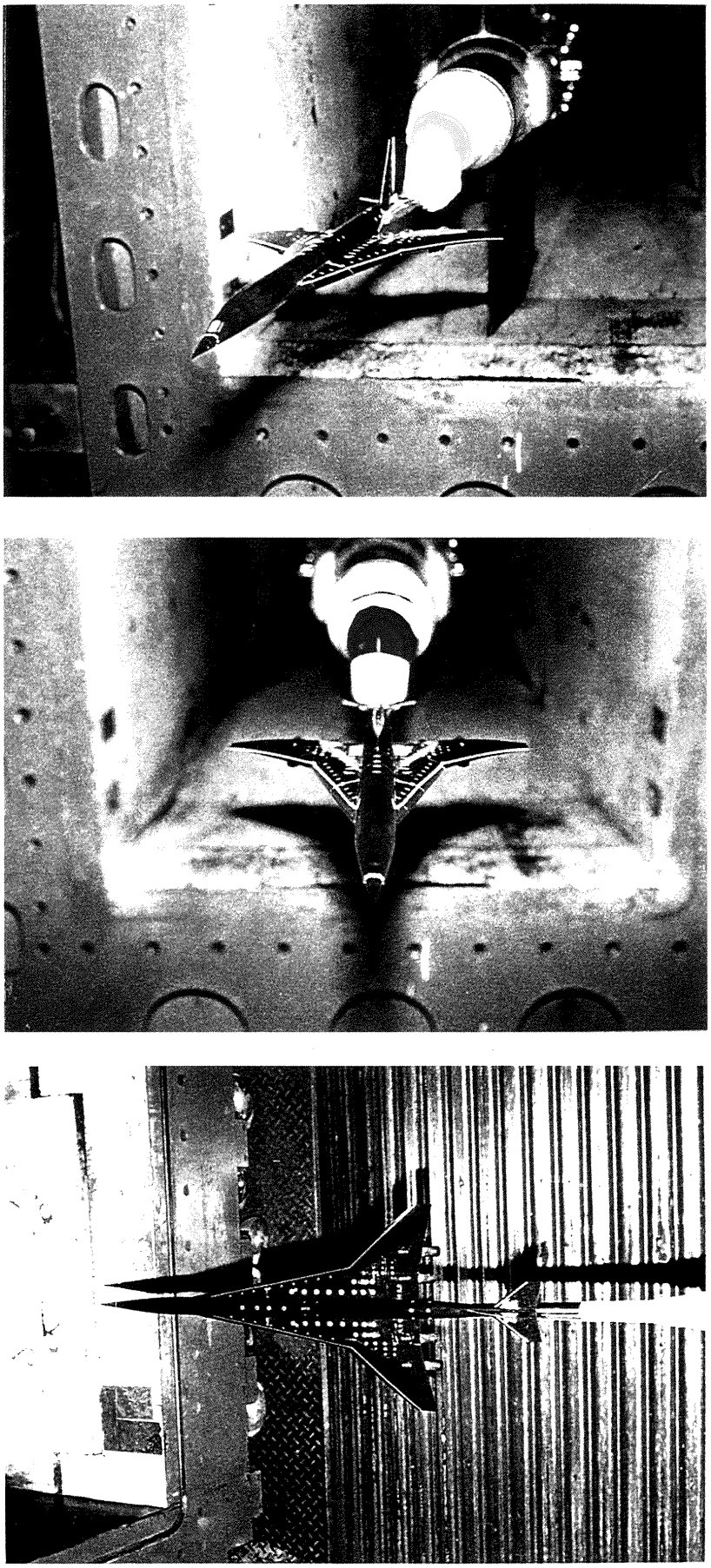

Figure 3 Model Installation Concept in Wind Tunnel

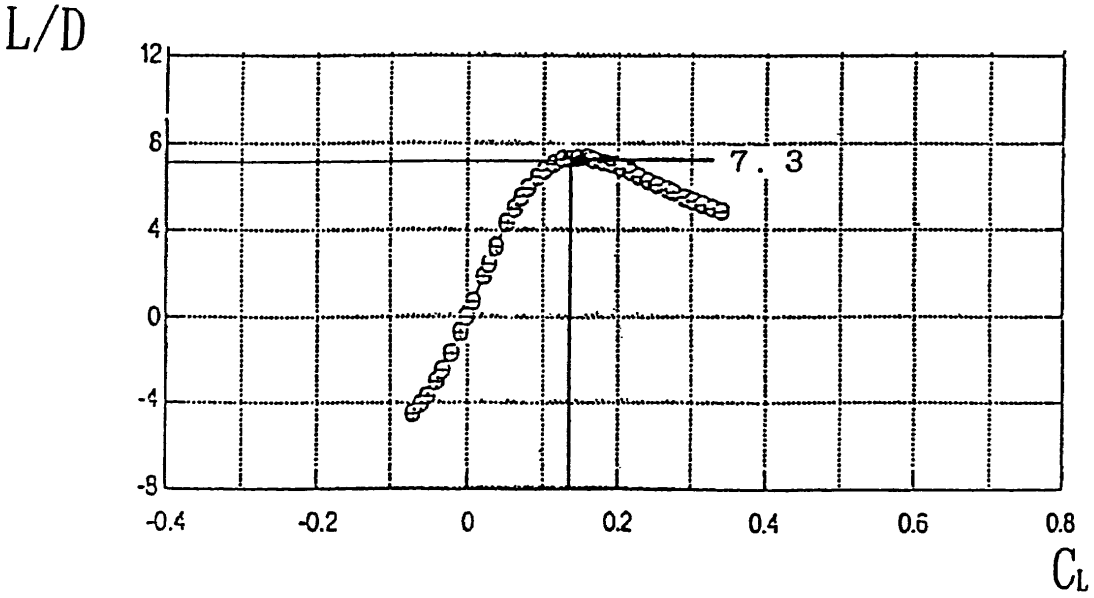

Figure 4 Lift to Drag Ratio(L/D) $\sim CL$ at $M = 2.0$

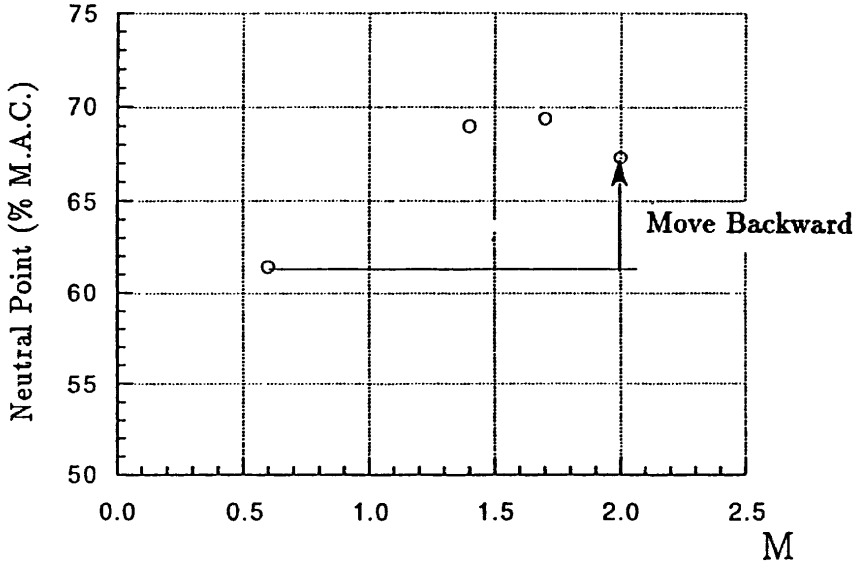

Figure 5 Neutral Point Variation at Various Mach Number

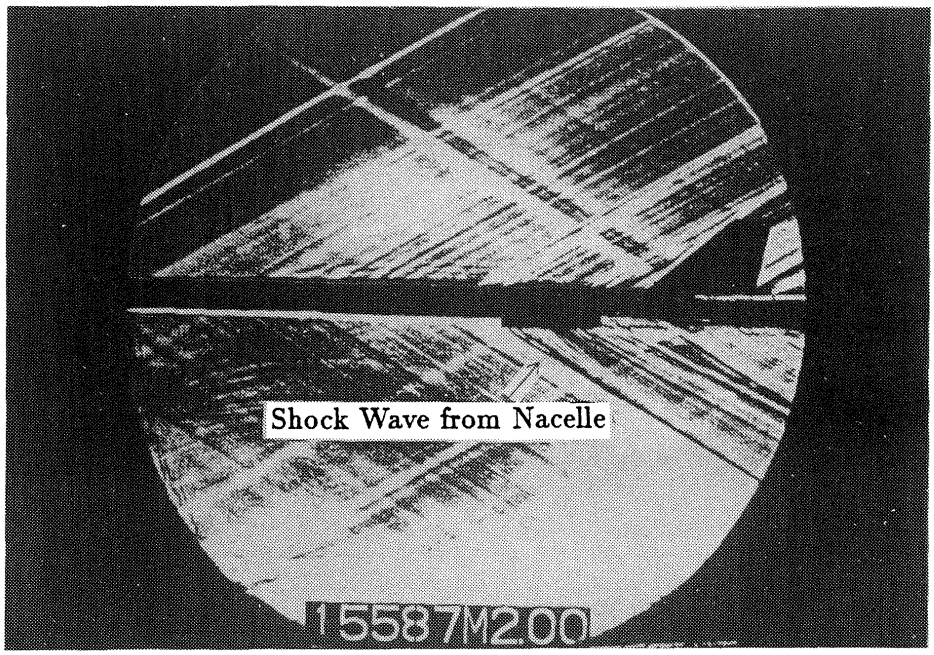

Figure 6 Schlieren Photograph at $M = 2.0$ and $\alpha \simeq 0°$

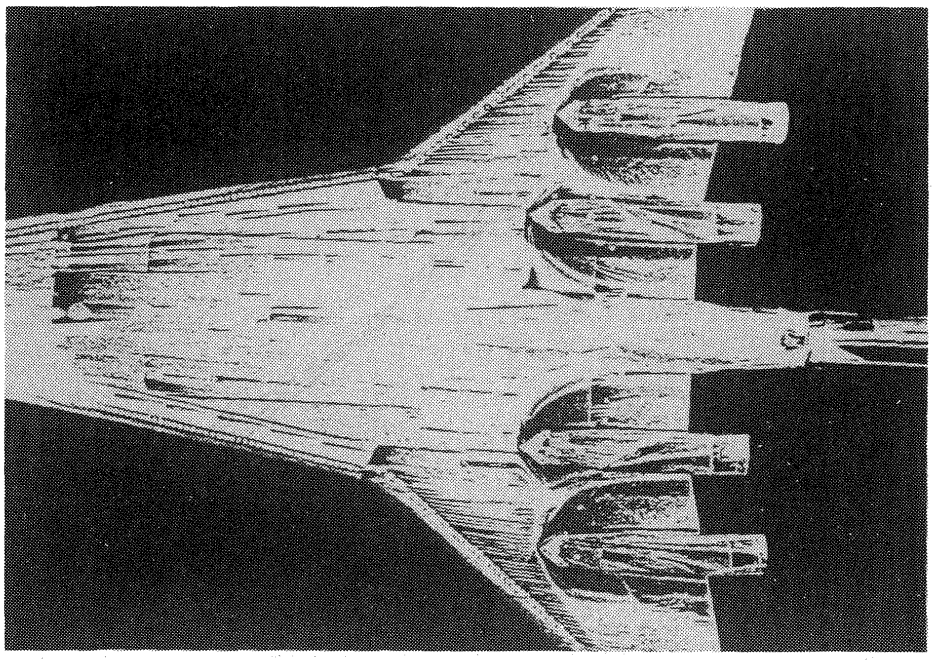

Figure 7 Oil Flow at M=2.0 and $\alpha = 0.8°$

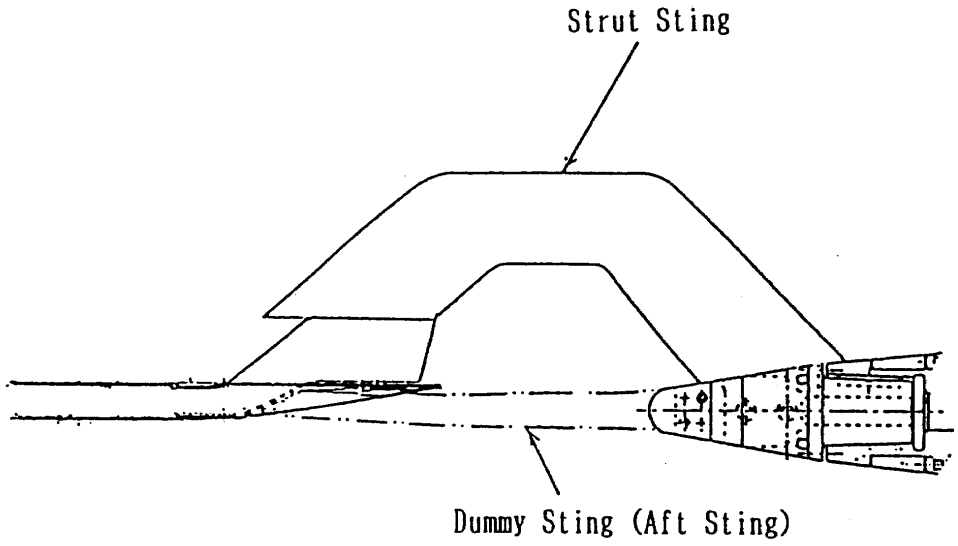

Figure 8 Model Supporting System

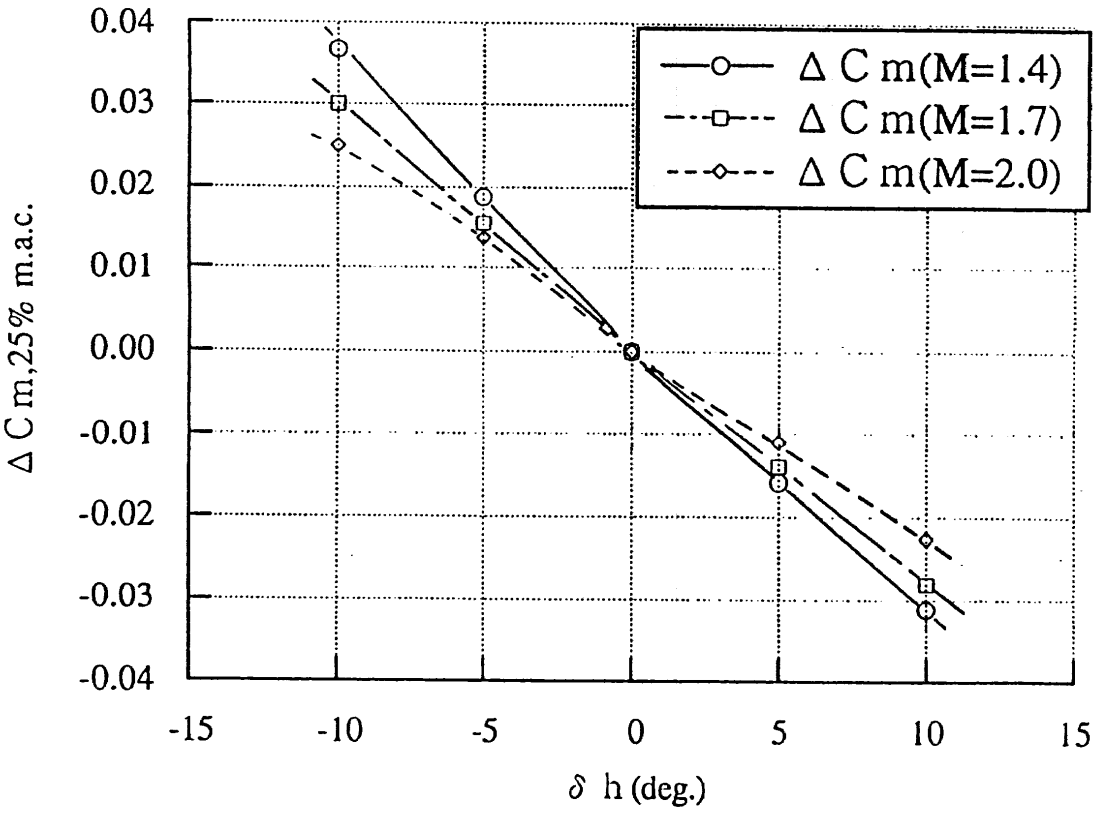

Figure 9 Effect of Stabilizer Deflection

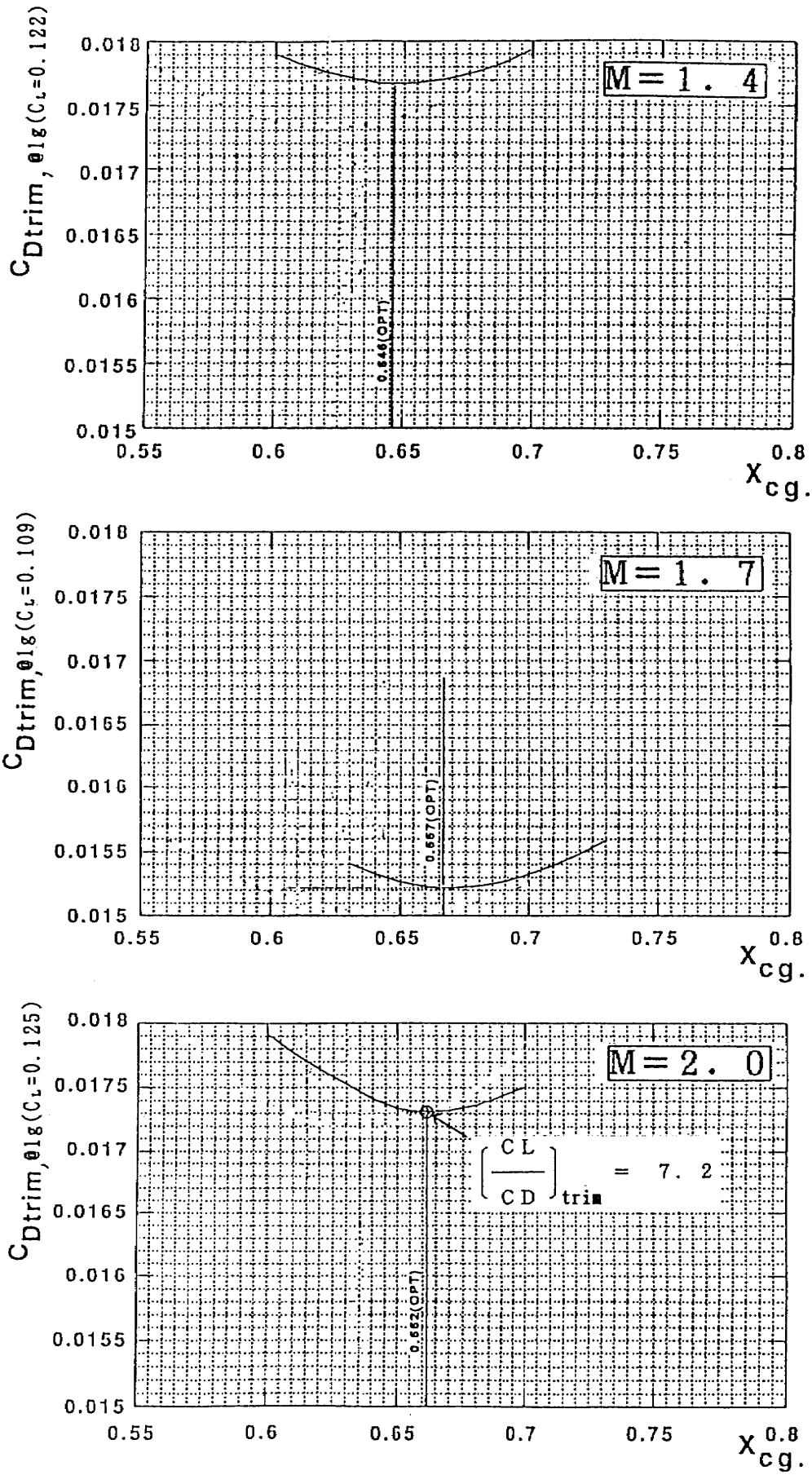

Figure 10 CD $_{trim}$ ~ Optimum Center of Gravity

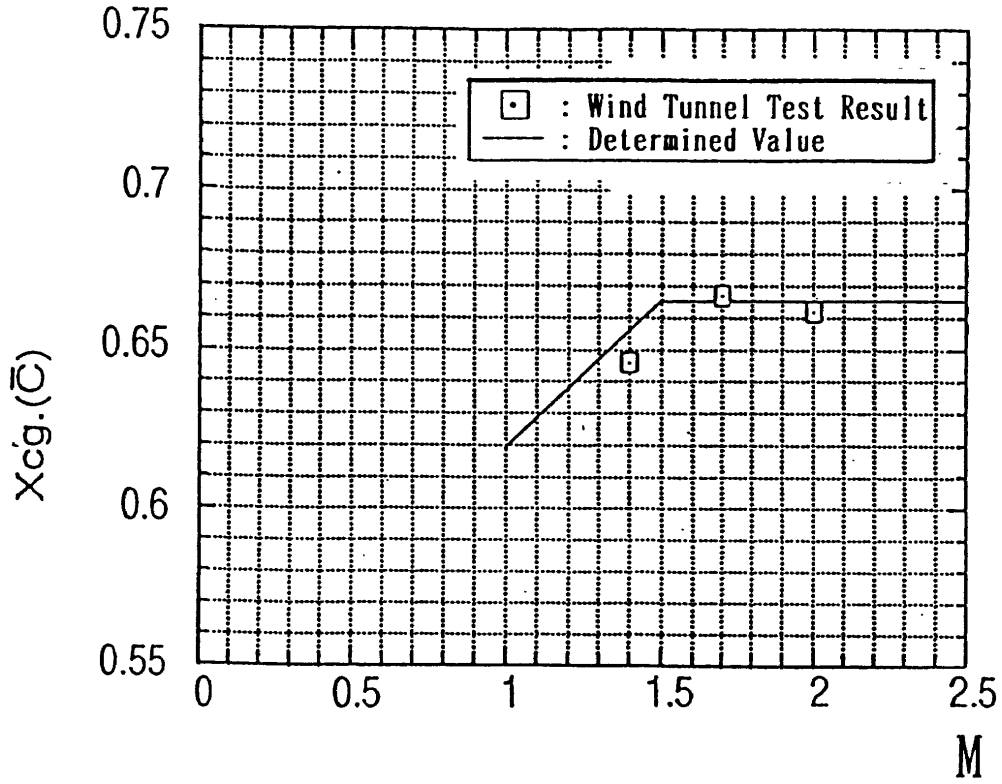

Figure 11 Determination of Optimum Center of Gravity

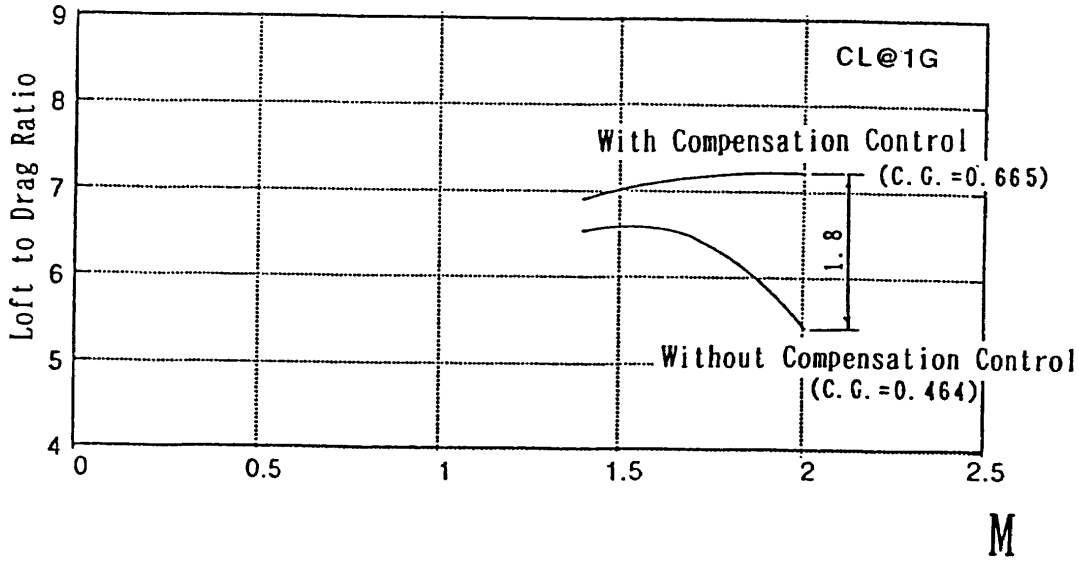

Figure 12 Effect of Longitudinal Stability Compensation Control for Lift to Drag

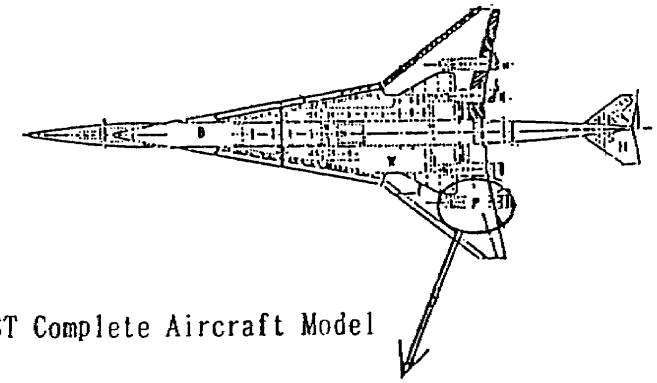

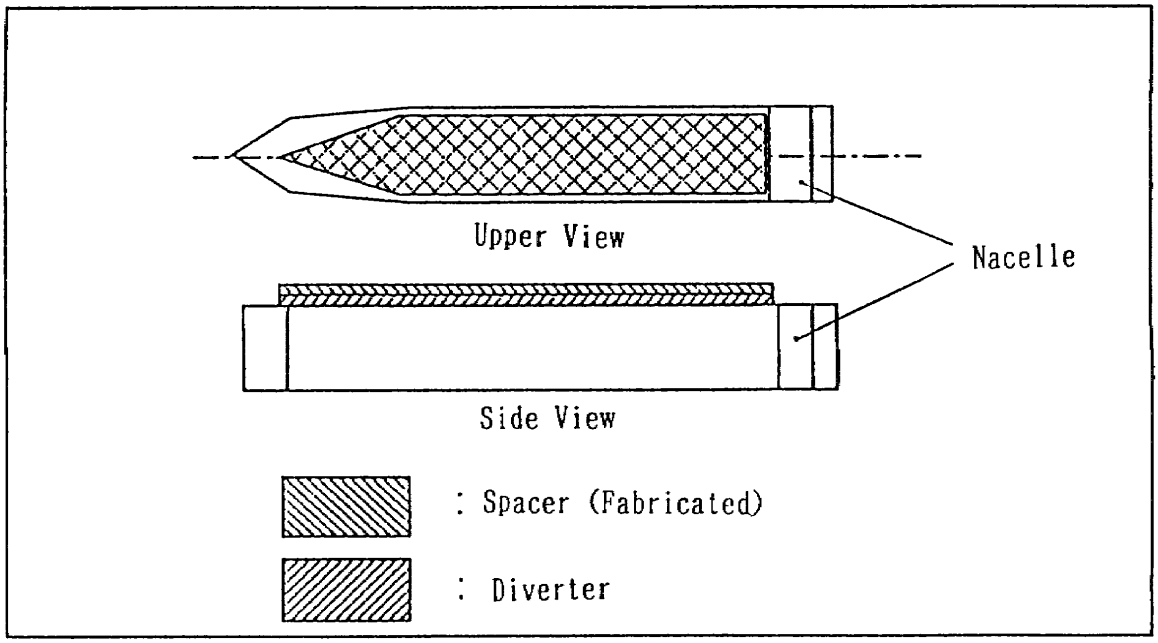

(a) Spacer Position

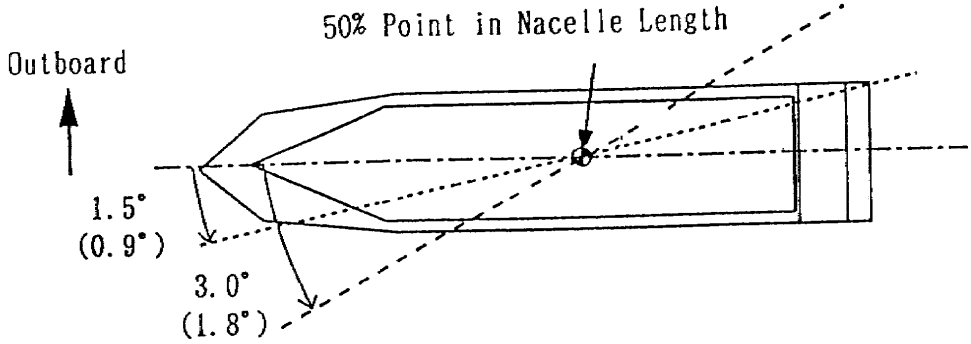

(b) Nacelle Azimuthal Angle (For Outboard Nacelle)
(Angles for the inboard nacelle are shown in parentheses.)

Figure 13 Fabricated Spacer

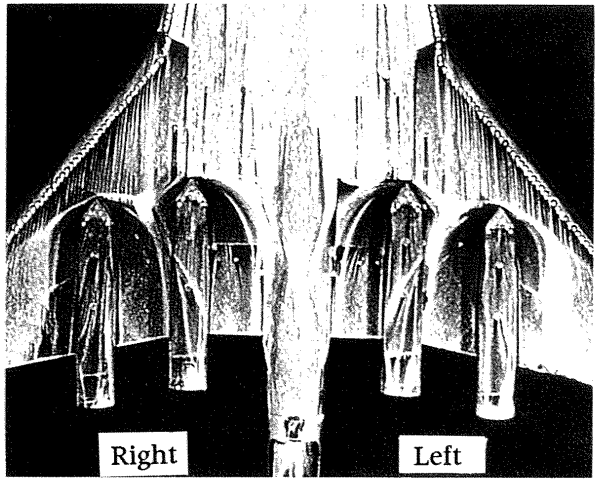

(a) Original Diverter Height
(Less than Boundary Layer Thickness δ)

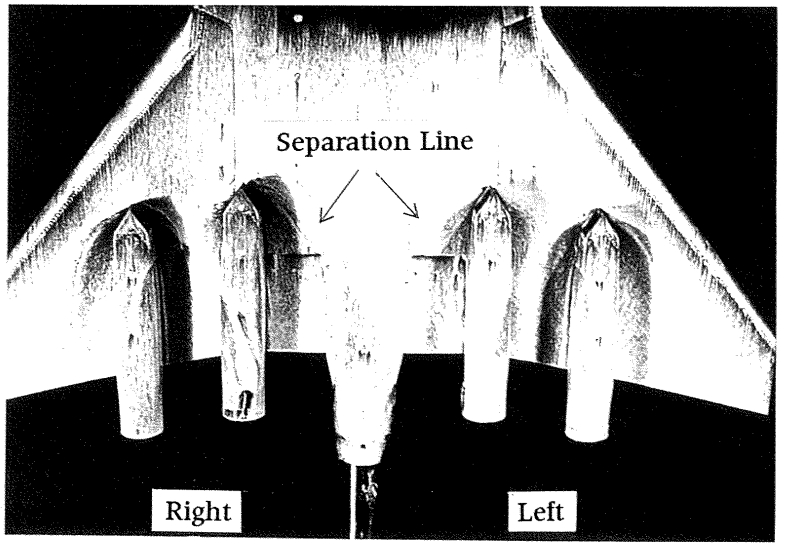

(b) Diverter Height of δ

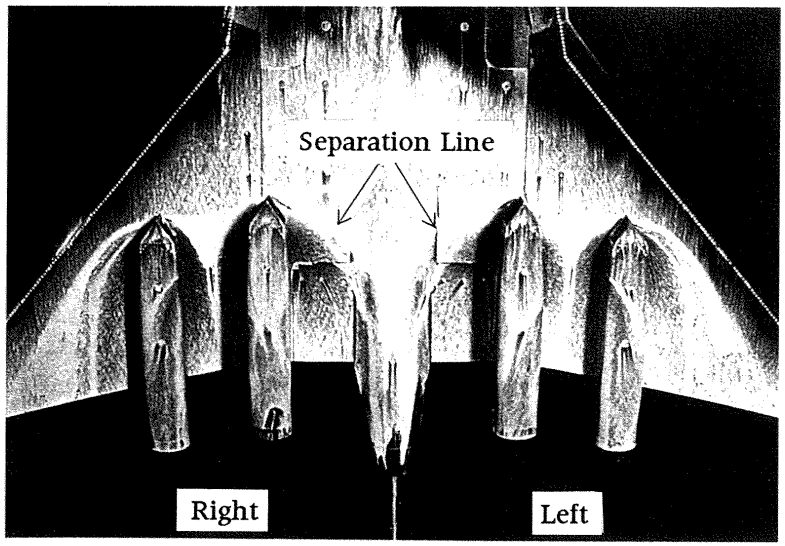

(c) Diverter Height of 5δ

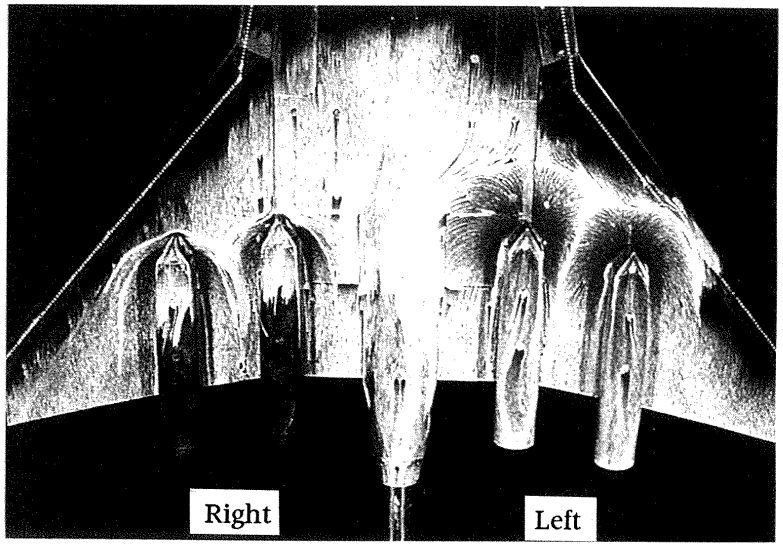

(d) Original Diverter Height (Left Nacelle Outlet is closed.)

Figure 14 Effect of Diverter Height on the Wing Surface in Oil Flow Photograph (Wing Under Surface)

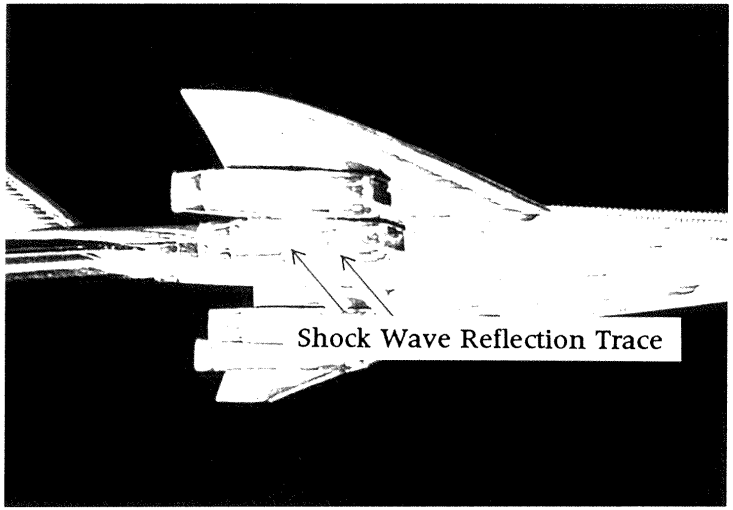

(a) Original Diverter Height
(Less than Boundary Layer Thickness δ)

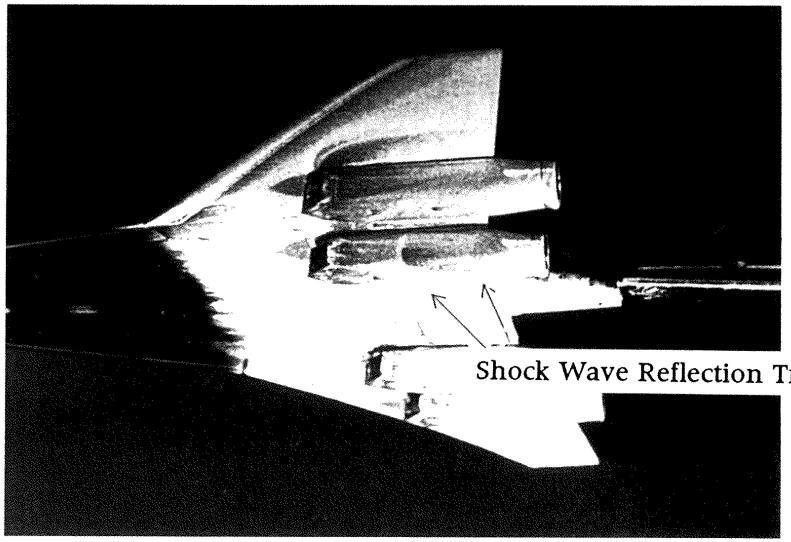

(b) Diverter Height of δ

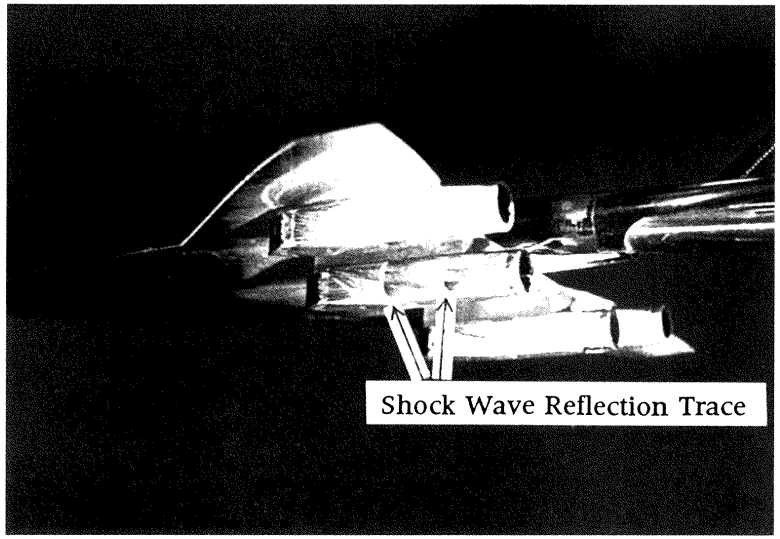

(c) Diverter Height of 5δ

Figure 15 Effect of Diverter Height on the Wing Surface in Oil Flow Photograph (Side of Nacelle)

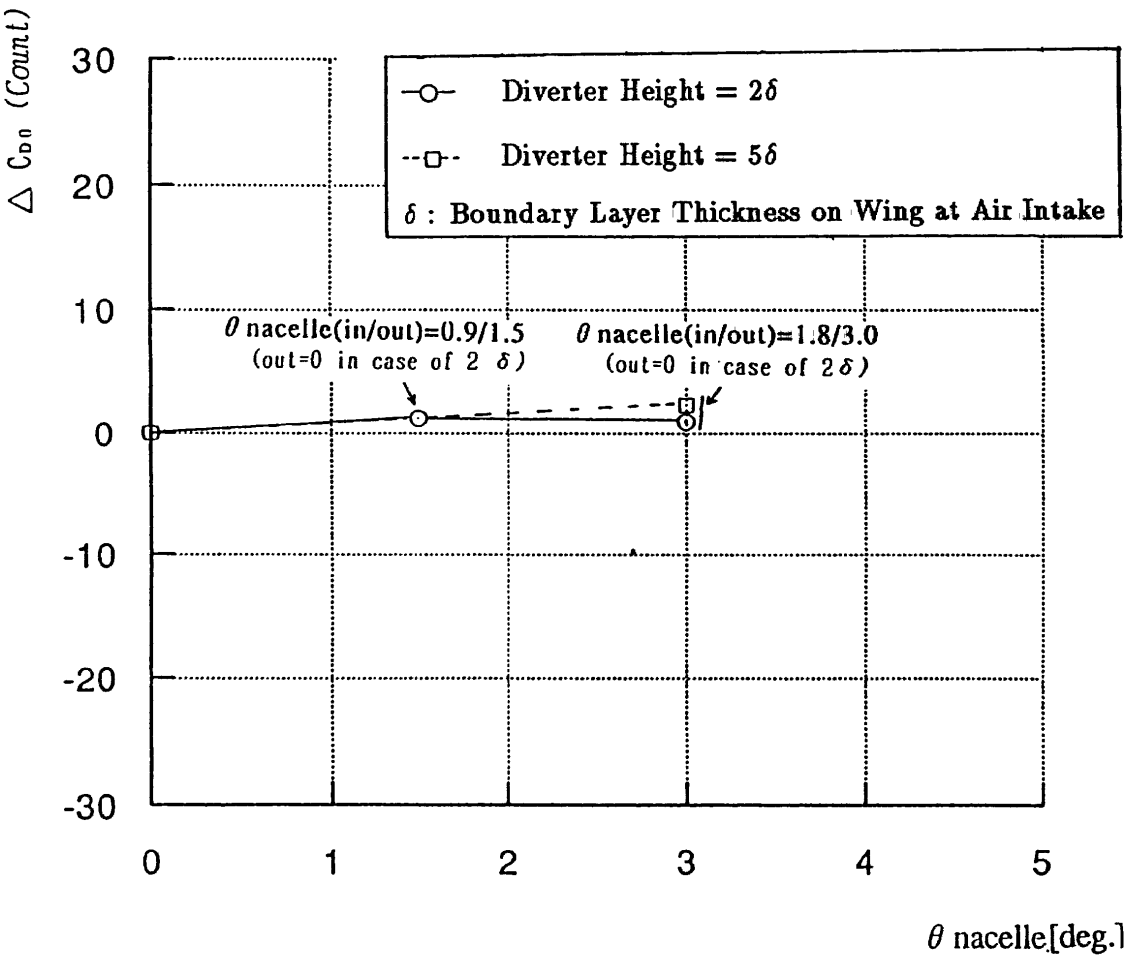

Figure 16 Effect of Change of Nacelle Azimuthal angle

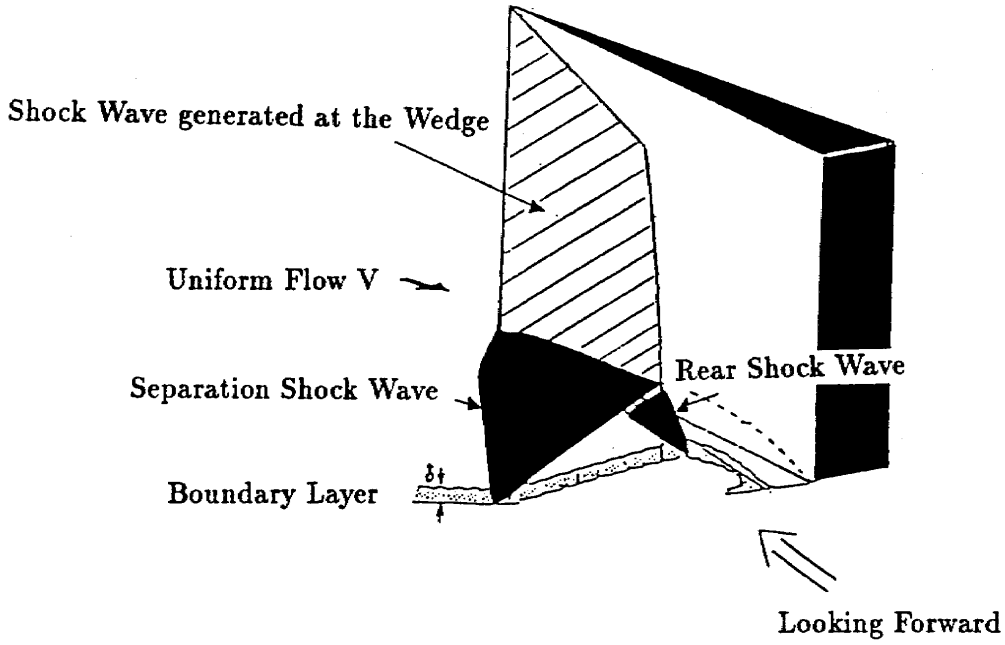

(a) Flow Field around a Wedge on a Flat Plate in Supersonic Speed Flow

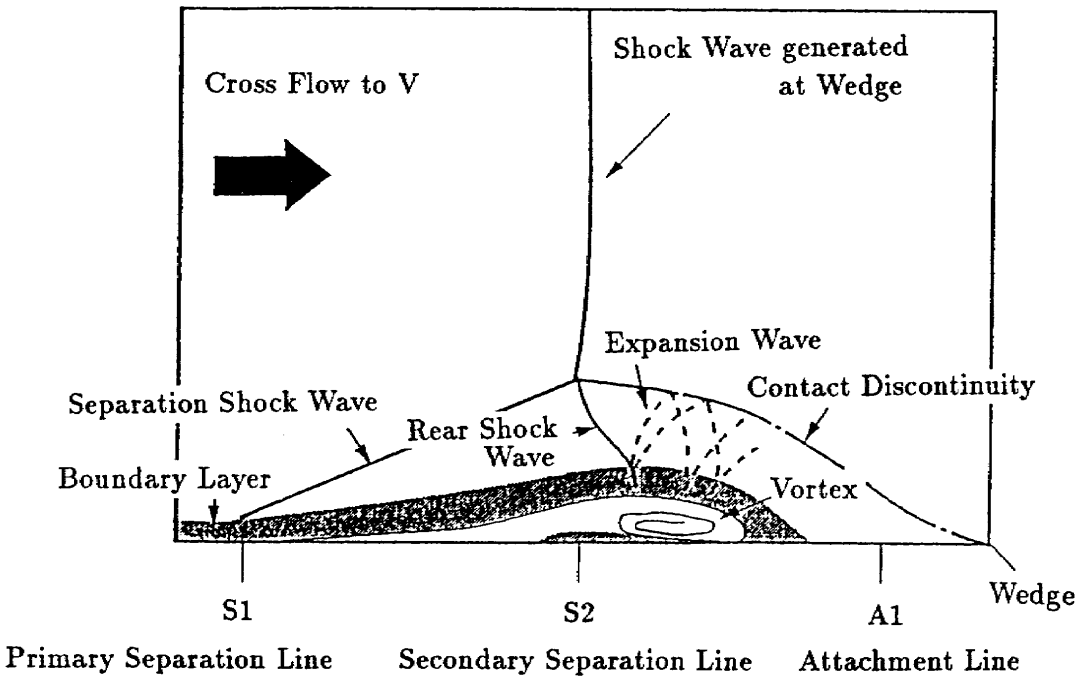

(b) Flow Field of Interaction between Shock Wave and Boundary Layer (Looking Forward of (a))

Figure 17 Conceptual Figure of Flow Field of Interaction between Shock Wave and Boundary Layer

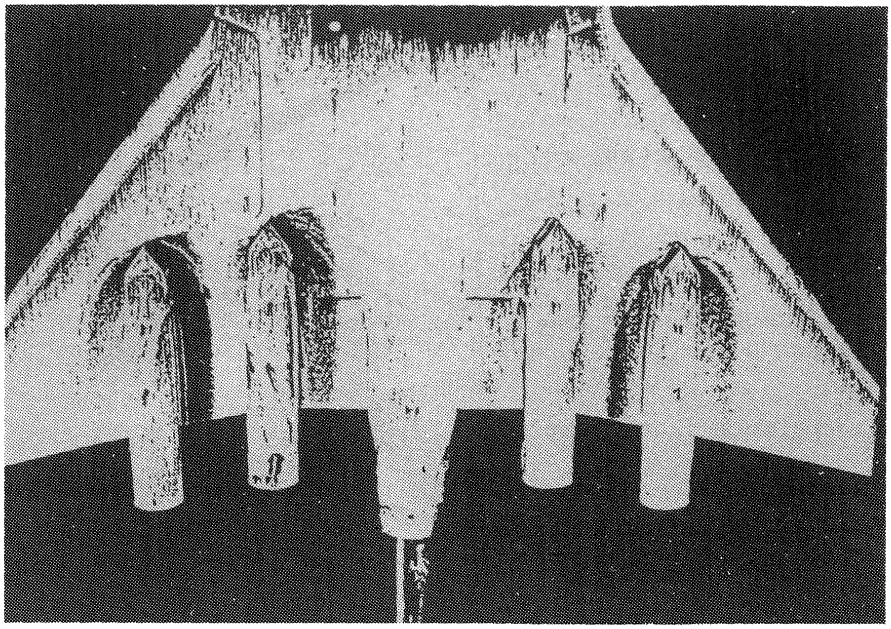

(a) Oil Flow Photograph

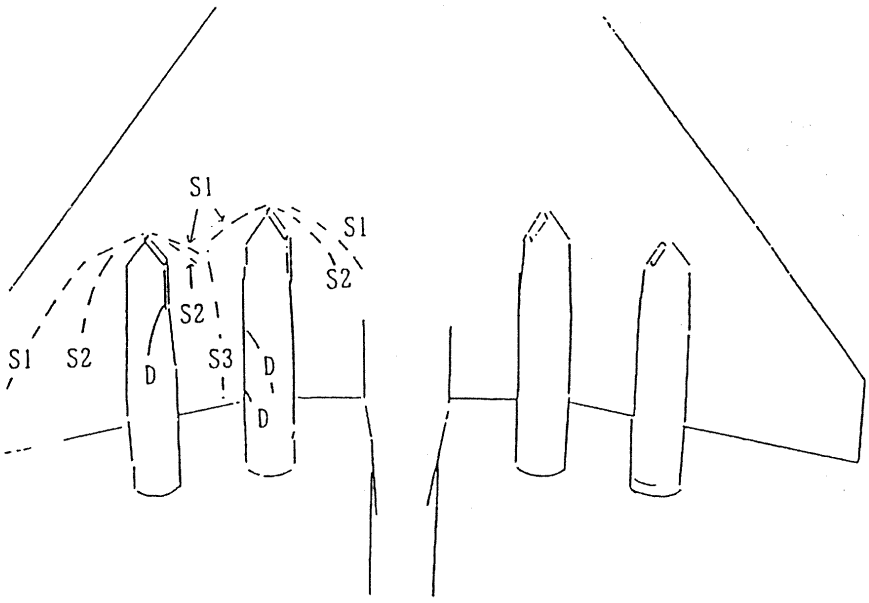

S1 : Primary Separation Line
S2 : Secondary Separation Line
S3 : Combined Separation Line of Primary and Secondary Separation Line
D : Shock Wave Trace

(b) Schematic of Oil Flow

Figure 18 Outline of Wing under Surface Flow Field

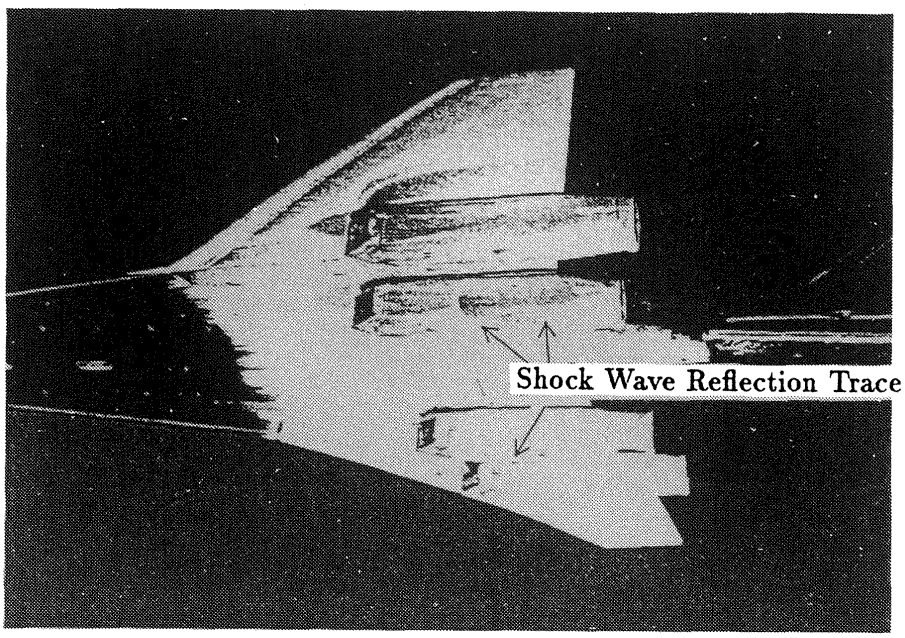

(a) Shock Wave Reflection Trace on Side of Nacelle

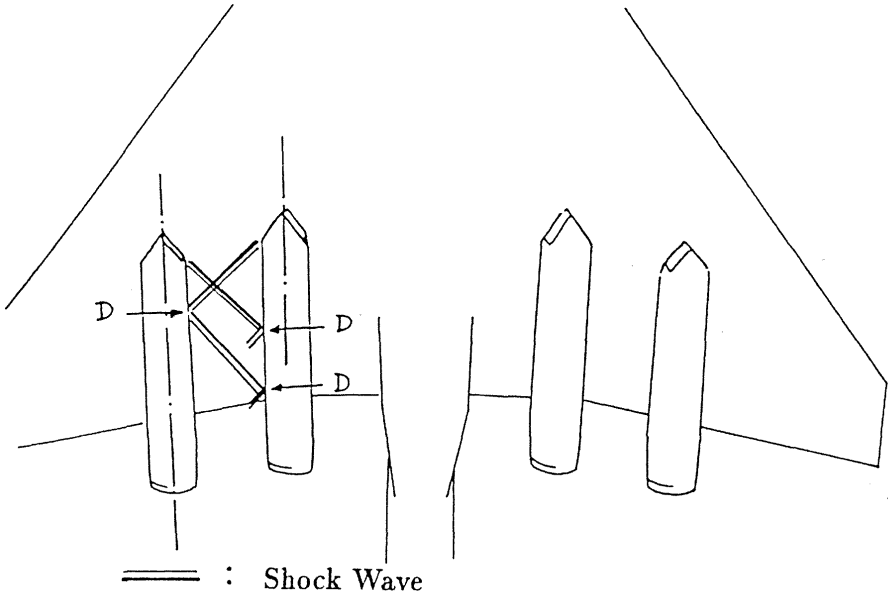

(b) Interaction of Shock Waves between Inboard and Outboard Nacelles

Figure 19 Outline of Flowfield on Side of Nacelle